J. Fluid Mech. (1986), *vol.* 163, *pp.* 1–20
Printed in Great Britain

A stability analysis of non-time-periodic perturbations of buoyancy-induced flows in pure water near 4 °C

By I. M. EL-HENAWY,
Department of Mathematics, Mansoora, University, Mansoora, Egypt

B. D. HASSARD AND N. D. KAZARINOFF
Department of Mathematics, State University of New York at Buffalo, N.Y. 14214 U.S.A.

(Received 1 February 1984 and in revised form 24 June 1985)

A new approach to determine stability of multiple steady-state similarity solutions corresponding to laminar flows is introduced and applied to laminar flows in cold, pure water at temperature T_∞ °C (near 4 °C) adjacent to a vertical, isothermal, plane surface at temperature T_0 °C when $0 < R \equiv (4-T_\infty)/(T_0-T_\infty) < 0.5$, the region of buoyancy-force reversals. The results show that the steady-state similarity solutions recently found in this region by El-Henawy *et al.* (1982) are unstable, and thus should not be observed experimentally; while those solutions found earlier by Carey, Gebhart & Mollendorf (1980) may be stable. No unstable modes corresponding to their solutions were found. Some flows for R in the range of strong buoyancy-force reversals, $0.14 < R < 0.32$ at Prandtl number $Pr = 11.6$, have been observed, for example at $R = 0.143, 0.254$ and 0.317 by Carey & Gebhart (1981) and Wilson & Vyas (1979). The latter found time-varying flows in this region of strongest flow reversals.

The advantages of the method introduced are reduction of mathematical shortcomings of the traditional approach and relative ease of numerical calculation of the real eigenvalues and eigenfunctions. The disadvantage is that information on downstream, selective frequency, exponential growth of amplitude is lost. The theory presented may be regarded as an asymptotic limit of the standard hydrodynamic theory as the frequency of perturbations approaches zero.

1. Introduction

The stability characteristics of boundary-layer flows in pure or saline water close to its temperature of maximum density T_m °C are of particular interest, for then the local temperature T °C of the water relative to T_m strongly influences the velocity and temperature profiles of the steady-state similarity solutions *and* the experimentally observed flows; see Wilson & Vyas (1979), Carey & Gebhart (1981), Sammakia (1981) and El-Henawy *et al.* (1982), and figure 1. For the similarity solutions corresponding to the laminar flow of cold, pure water adjacent to an isothermal, semi-infinite flat plate (see figure 2) this occurs for $R \equiv (T_m-T_\infty)/(T_0-T_\infty)$ close to either 0.151 or 0.292. For $T_0 = 0$ °C and $T_m = 4.029325$ °C this means that the initial temperature of still, cold, pure water is close to either 4.7460 °C or 5.6911 °C. Moreover, for R in each of the ranges (0.15148, 0.15180) and (0.29181, 0.45402), corresponding to T_∞ in the ranges (4.74865 °C, 4.75044 °C) and (5.6886 °C, 7.3800 °C), multiple solutions of the similarity equations were found by El-Henawy *et al.* (1982). Some pairs of these

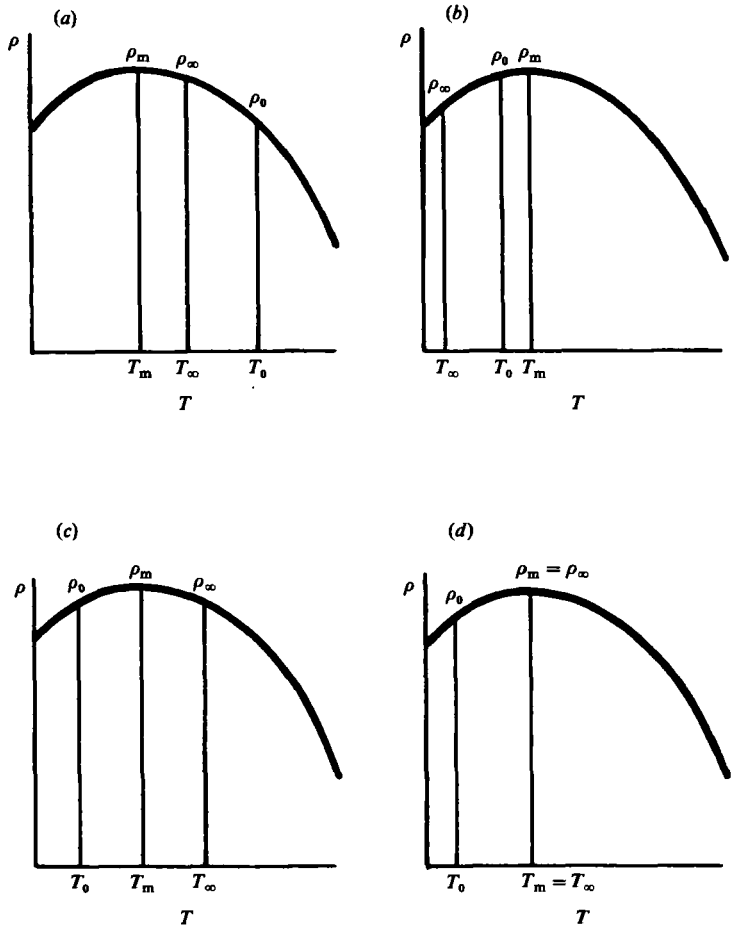

FIGURE 1. The effect of specified temperatures T_0 and T_∞ on R, on the buoyancy force $B(T)$ and on flow direction. T_0, T_∞ and T_m are the temperatures of the isothermal plate, of the ambient water, and at which water has maximum density. The subscripted variables ρ are the corresponding densities. (*a*) $B > 0$, $R < 0$, and the flow is up; (*b*) $B < 0$, $R > 0$, and the flow is down; (*c*) $B \leqslant 0$, $R = \frac{1}{2}$, and the flow is down; and (*d*) $B > 0$, $R = 0$, and the flow is up.

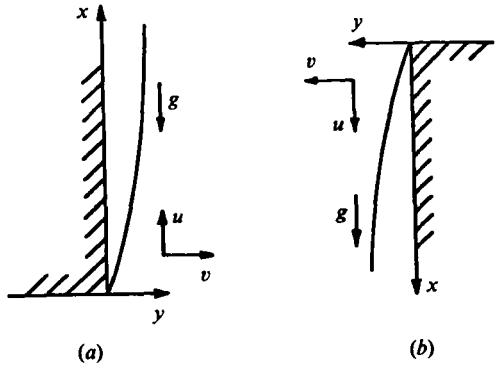

FIGURE 2. The coordinate systems: (*a*) upflow, (*b*) downflow.

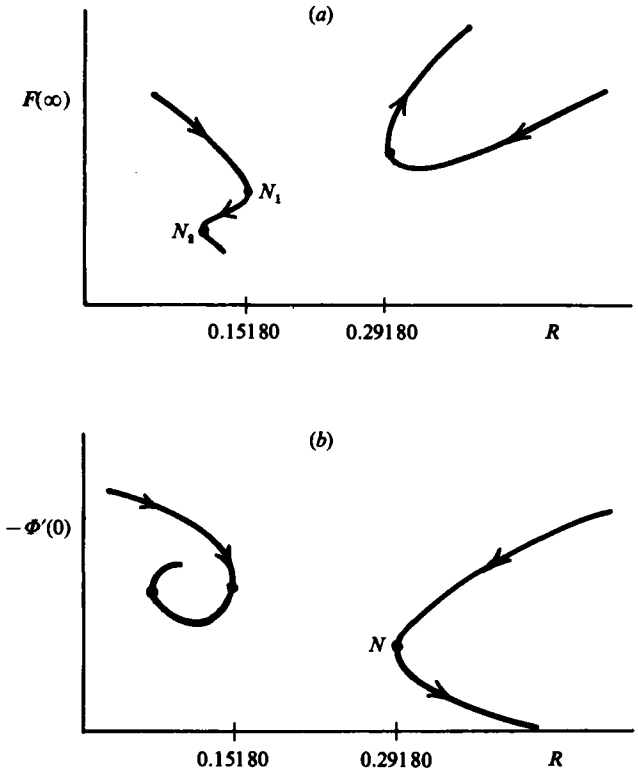

FIGURE 3. Variation of $F(\infty)$ and $-\Phi'(0)$ with R (base flows).

existing at the same $R > 0.292$ have distinctly different velocity and temperature profiles, including vastly different heat-transfer rates at the vertical surface. If flows with dramatically low heat-transfer rates are observable in the laboratory, then it might be possible to take advantage of the conditions that cause them in technological applications. Both Wilson & Vyas (1979) and Carey & Gebhart (1981) observed flows in the range (5.69 °C, 7.38 °C), for example at 5.9 °C. Wilson & Vyas wrote 'It is noted that oscillations become appreciable exactly within the dual flow regime...'. Carey & Gebhart found the flow to depart from numerical predictions at 4.7 °C except close to the ice wall.

In view of the uncertainties about the nature of the flows of pure water in the region of strong buoyancy-force reversals (4.7–7.38 °C) and the numerical discovery of multiple steady-state solutions in this range, both more experimental work and analysis are needed. The stability of the multiple steady-state solutions, which has not been studied previously, and the implications the results have for actual flows are the object of our investigation. As will be seen, the approach we follow is widely applicable to problems for which multiple steady-state solutions are found. In brief, our results indicate that the solutions with strong velocity reversals and very low heat-transfer rates are not stable in time to small perturbations. Our results for the stability of laminar, steady-state flows of cold, pure water adjacent to a vertical, semi-infinite, flat, isothermal surface (hereafter called Problem S) are best described in terms of bifurcation diagrams for the two known families of steady-state solutions $(F(\eta), \Phi(\eta))$ of (1.7) below, one existing for $R < 0.1518$ (largely upflow), the other existing for $R > 0.2918$ (largely downflow), see figure 3 (a, b). We show in §2 that the

steady-state solutions, which exist for $R < 0.1518$ and which correspond to points $(R, F(\infty))$ in the bifurcation diagram 3(*a*) with $F(\infty)$ below its value (approximately 0.045) at N_1, are unstable (at least one eigenvalue of the associated linear system (1.9) below is positive). We believe that those solutions corresponding to points with $F(\infty)$ above its value at N_1 may be stable (we found no eigenvalue λ that is positive there). We also show in §2 that the steady-state solutions, which exist for $R > 0.291$ and which correspond to points $(R, -\Phi'(0))$ in the bifurcation diagram figure 3(*b*) with $-\Phi'(0)$ below its value (approximately 0.493) at N, are unstable (we found one positive λ), and those with $\Phi'(0)$ above its value at N may be stable (we found no positive λ there).

For the family of solutions that exists for $R < 0.16$, we found three eigenvalues $\lambda = \lambda_i(R, F(\infty))$ with eigenvectors $(f_i(\eta), \phi_i(\eta))$ $(i = 1, 2, 3)$. For $i = 1$ and 2, $\lambda_i(R, F(\infty))$ changes its algebraic sign at the nose N_i in figure 3(*a*). We did not find a third nose N_3 at which $\lambda_3(R, F(\infty))$ changes its algebraic sign, but we conjecture that such a nose exists.

Among the many previous experimental or numerical studies of Problem S (including various fluids and either a uniform flux or isothermal boundary condition) are those by Nachtsheim (1963), Polymeropoulos & Gebhart (1967), Knowles & Gebhart (1968), Dring & Gebhart (1968, 1969), Gill & Davey (1969), Vliet & Liu (1969), Jaluria & Gebhart (1974), Gebhart (1979), Qureshi (1980), Higgins (1981), and (a contemporary study) Hwang, Kazarinoff & Mollendorf (1984). Nachtsheim made a thorough and skilful analysis of the isothermal-plate problem in the Boussinesq case (buoyancy force linear in T). The experimental results of Polymeropoulos & Gebhart confirmed Nachtsheim's numerical results within reasonable limits. Qureshi was the first to compute neutral-stability curves using the nonlinear buoyancy-force function of Gebhart & Mollendorf (1977). He did this for the no-flux boundary condition for saline water at $R = 0$ and compared the results with experimental data. Higgins computed the neutral-stability curve and contours of constant amplification at $R = 0.4$ for Problem S. She also verified, within rough limits, her theoretical results with experiments. Hwang *et al.* determined neutral-stability curves of the same problem for $0.29181 < R < 0.34$ and found that, as one descends to below the nose N in figure 3(*b*), the corresponding solutions are amplified ever closer to the leading edge of the plate. All the numerical analyses cited above have implemented what we call here the traditional or conventional approach to hydrodynamic stability (Drazin & Reid 1981; Lin 1955).

Our approach is distinctly different from the conventional one, as will be seen below. The Problem S studied here is the stability of steady-state, similarity solutions of the Navier–Stokes-energy system

$$\rho(u_x + v_y) = 0, \tag{1.1a}$$

$$u_t + uu_x + vu_y = -\frac{1}{\rho}p_x + \nu\,\Delta u + B(T), \tag{1.1b}$$

$$v_t + uv_x + vv_y = -\frac{1}{\rho}p_y + \nu\,\Delta v, \tag{1.1c}$$

$$T_t + uT_x + vT_y = \tilde{\alpha}\,\Delta T, \tag{1.1d}$$

$$u(x,0,t) = v(x,0,t) = T(x,0,t) - T_0 = T(x,\infty,t) - T_\infty = u(x,\infty,t) = 0, \tag{1.1e}$$

where T is the temperature at (x, y, t), $B(T)$ denotes buoyancy force, x and y are coordinates respectively parallel and perpendicular to the vertical, isothermal surface $y = 0$ (see figure 2), t is time, u and v are respectively the vertical and horizontal

components of fluid velocity at (x, y, t), p is the motion pressure at (x, y, t) and ρ is the (constant) density of pure water at temperature T.

The buoyancy force $B(T)$ has been fitted to data by Gebhart & Mollendorf (1977) to within 3.5 p.p.m. accuracy for pure water. In terms of

$$\phi = \frac{T-T_\infty}{T_0-T_\infty}, \quad W(\phi, R) = [|\phi-R|^q - |R|^q]\,|T_0-T_\infty|^q, \tag{1.2}$$

their formulation is

$$B(T) = \mp g\alpha W(\phi, R), \tag{1.3}$$

where for pure water at 1 bar

$$q = 1.894816, \quad \alpha = (9.297173\times 10^{-6}\ ^\circ\mathrm{C})^q \quad \text{and} \quad T_\mathrm{m} = 4.029325\ ^\circ\mathrm{C}.$$

Also, $g = 9.81\ \mathrm{m/s^2}$, and $\nu \simeq 1.67\times 10^{-6}\ \mathrm{m^2/s}$. In (1.3) the + sign is used for base (steady-state) flows that are largely upflow (see figures 1*a* and 2*a*) which occur for $R \leqslant 0.151\,80$, and the − sign is used for base flows that are largely downflow (see figures 1*b* and 2*b*) which occur for $R \geqslant 0.291\,81$.

We begin our analysis of Problem S for (1.1), with $B(T)$ as in (1.23), by making a similarity transformation from (x, y, t) to (η, τ) defined by

$$\eta(x, y) = \frac{yG}{4x}, \quad \tau = C_1 x^{-\frac{1}{2}} t, \tag{1.4}$$

where C_1 is a constant to be determined later, which will non-dimensionalize τ, and the Grashof number G is defined to be

$$G = 4[\tfrac{1}{4} Gr(x, T_\infty)]^{\frac{1}{4}}$$

with

$$Gr(x, T_\infty) = \frac{\alpha g}{\nu^2} x^3\,|T_0-T_\infty|^q. \tag{1.5}$$

We also choose a stream function ψ so that, as usual, $u = \psi_x$ and $v = -\psi_y$. In addition to ϕ, given by (1.2), we define new dependent variables f and P in terms of (η, τ) by

$$\psi(x, y, t) = \nu G f(\eta, \tau), \quad P(\eta, \tau) = \rho\left(\frac{4x}{\rho\nu G}\right)^2 p(x, y, t). \tag{1.6}$$

We rewrite (1.1) in terms of these new dependent and independent variables and in writing each equation we neglect terms of order G^{-2} compared with other terms in the same equation, exactly as was done by El-Henawy *et al.* (1982). In the traditional approach the parallel-flow hypothesis is used, and terms of order $1/G$ are neglected; see Hieber & Gebhart (1971). The truncated similarity equations, which are derived from (1.1) using (1.2)–(1.5), are:

$$f_{\eta\tau} + 2f_\eta^2 - 3ff_{\eta\eta} + 2\tau\{f_{\eta\eta} f_\tau - f_\eta f_{\eta\tau}\} = f_{\eta\eta\eta} \pm \{|\phi-R|^q - |R|^q\}, \tag{1.7a}$$

$$\begin{aligned} f_\tau - \eta f_{\eta\tau} - 2\tau f_{\tau\tau} + 9ff_\eta - \eta f_\eta^2 - 3\eta ff_{\eta\eta} - 4\tau f_\tau f_\eta - 4\tau^2 f_{\tau\tau} - 2\eta\tau\{f_{\eta\tau} f_\eta - f_{\eta\eta} f_\tau\} \\ = -P_\eta + \eta f_{\eta\eta\eta} - f_{\eta\eta} + 6\tau ff_{\eta\tau} - 4\tau^2 f_\tau f_{\eta\tau} + 2f_{\eta\eta\tau}, \end{aligned} \tag{1.7b}$$

$$Pr(-3f\phi_\eta + \phi_\tau - 2\tau\{\phi_\tau f_\eta - f_\tau \phi_\eta\}) = \phi_{\eta\eta}, \tag{1.7c}$$

with boundary conditions

$$f(0, \tau) = f_\eta(0, \tau) = \phi(0, \tau) - 1 = 0, \quad f_\eta(\infty, \tau) = \phi(\infty, \tau) = 0, \quad P(\infty, \tau) = 0. \tag{1.7d}$$

In (1.7*c*) $Pr \equiv \nu/\tilde{\alpha}$ is the Prandtl number, chosen to be 11.6 throughout. We have also chosen $C_1 = \frac{1}{2}[g\alpha\,|T_0-T_\infty|^q]^{\frac{1}{2}}$. This non-dimensionalizes τ and makes the coefficient

of the buoyancy-force term in (1.7*a*) equal to 1. We note that, once ϕ and f are found from (1.7*a*, *c*, *d*), then (1.7*b*) can be integrated with respect to η to determine P. The constant of integration P is proportional to $F(\infty)$. We set (1.7*b*) aside for the remainder of this paper.

Our next step is to linearize (1.7) about a steady-state solution (F, Φ) whose stability we seek to study. To do this we specify our class of perturbations; namely, we choose

$$f(\eta,\tau) = F(\eta)+\epsilon e^{\lambda\tau}\tilde{f}(\eta), \quad \phi(\eta,\tau) = \Phi(\eta)+\epsilon^{\lambda\tau}\tilde{\phi}(\eta), \tag{1.8}$$

where ϵ is positive and small. We replace f and ϕ in (1.7) by the right-hand members of (1.8), divide by ϵ, let $\epsilon\to 0$, and divide by $e^{\lambda\tau}$. The result is the following linear system of fifth order for $(\tilde{f}, \tilde{\phi})$:

$$\lambda\tilde{f}_\eta+2\lambda\tau\{F_{\eta\eta}\tilde{f}-F_\eta\tilde{f}_\eta\} = \tilde{f}_{\eta\eta\eta}+3(F_{\eta\eta}\tilde{f}+F\tilde{f}_{\eta\eta})-4F_\eta\tilde{f}_\eta\pm q\,\mathrm{sign}\,(\Phi-R)\,(|\Phi-R|^{q-1}\tilde{\phi}), \tag{1.9a}$$

$$Pr[\lambda\tilde{\phi}-2\lambda\tau(F_\eta\tilde{\phi}-\Phi_\eta\tilde{f})-3(F\tilde{\phi}_\eta+\Phi_\eta\tilde{f})] = \tilde{\phi}_{\eta\eta}, \tag{1.9b}$$

with boundary conditions

$$\tilde{\phi}(0) = \tilde{f}(0) = \tilde{f}_\eta(0), \quad \tilde{f}_\eta(\infty) = \tilde{\phi}(\infty) = 0.$$

We seek to solve this fifth-order system for real eigenvalues λ and real eigenvectors $(\tilde{f}, \tilde{\phi})$.

As is the case when following the traditional approach, the linear eigenvalue problem that we have obtained above is not well posed; τ appears explicitly in the coefficients. However, we fix τ and proceed to solve (1.9) just as in the conventional approach one fixes x, which appears in the coefficients of the linear system to be solved, and proceeds. We tested the solutions for their sensitivity to τ, and found that both the eigenvalues and eigenvectors obtained were not sensitive to changes in τ for $0 \leqslant \tau \leqslant 200$; see tables 1 and 2.

We close this section by making a comparison between the two approaches to solving Problem S and suggesting some possible other applications of ours. Although we neglect terms of order G^{-2} and do not invoke the parallel-flow hypothesis, our approach has the disadvantages that it is still not mathematically rigorous and downstream amplification of disturbances at a rate dependent upon the frequency of the disturbance is lost (cf. Gebhart 1969; Haaland & Sparrow 1973). However, there are off-setting advantages. The first is a general one. The stability system (1.9) which we obtain for real-valued perturbations is of order six after one adds the trivial equation $\lambda_\eta = 0$ and a sixth (normalizing) boundary condition. Following the traditional approach, one uses complex-valued perturbations and obtains a real-valued system of order 12. In addition, there are three parameters to be found: a real 'frequency' β, a disturbance 'wavenumber' $\mathrm{Re}\,(\alpha)$ and a downstream 'growth rate' $\mathrm{Im}\,(\alpha)$. If $\mathrm{Im}\,(\alpha)$ and x are fixed, it is difficult to solve the system of order 14 numerically over the range of R desired; see, for example, Hwang *et al.* (1985). This is so because, in the case at issue, (i) it is necessary to solve the stability equations on intervals $(0, \eta)$ over which the base flows have been accurately computed, and this means value of $\eta = 200$ for R close to 0.151 or 0.292; and (ii) the linear-stability problem is troublesome to solve when of high order because the boundary conditions are nearly all homogeneous. In computing the new stationary solutions El-Henawy *et al.* (1982) found that much larger values of η were required than those used by Carey *et al.* (1980) to compute base flows. Moreover, in previous studies using the technique of fitting asymptotic tails, Hieber & Gebhart (1971), Qureshi (1980)

τ	$\lambda_1(0.151775, 0.050)$	$\lambda_1(0.151788, 0.042)$
0	-0.321907×10^{-2}	0.232845×10^{-2}
0.5	-0.319652×10^{-2}	0.230691×10^{-2}
1.0	-0.317417×10^{-2}	0.228580×10^{-2}
2.0	-0.313005×10^{-2}	0.224476×10^{-2}
5.0	-0.300457×10^{-2}	0.213045×10^{-2}
10.0	-0.281576×10^{-2}	0.196477×10^{-2}
20.0	-0.249280×10^{-2}	0.170252×10^{-2}
50.0	-0.183688×10^{-2}	0.122124×10^{-2}
100.0	-0.126613×10^{-2}	0.834114×10^{-3}
150.0	-0.972309×10^{-3}	0.714213×10^{-3}
200.0	-0.777365×10^{-3}	0.512604×10^{-3}

TABLE 1. The dependence of the eigenvalue λ_1, evaluated at $R = 0.151775$, $F(\infty) = 0.05$, upon τ (column 2), and the dependence of the same eigenvalue λ_1 evaluated at $F(\infty) = 0.042$, $R = 0.151788$ upon τ (column 3). All computations done at $\eta_\infty = 200.0$.

τ	$\mu(0.291829, 0.5)$	$\mu(0.291897, 0.48)$
0	-0.385432×10^{-2}	0.695293×10^{-2}
0.5	-0.386239×10^{-2}	0.703256×10^{-2}
1.0	-0.388972×10^{-2}	0.720093×10^{-2}
5.0	-0.396233×10^{-2}	0.756245×10^{-2}
10.0	-0.409314×10^{-2}	0.758521×10^{-2}
50.0	-0.423932×10^{-2}	0.762839×10^{-2}
100.0	-0.439322×10^{-2}	0.771003×10^{-2}
200.0	-0.401239×10^{-2}	0.763994×10^{-2}

TABLE 2. The variation of $\mu(R, -\Phi'(0))$ with τ for two points $(R, -\Phi'(0))$ near to N in figure 3

and Higgins (1981) integrated in from η with $\eta = 14$ or 20 (Hieber & Gebhart), $\eta = 8$ (Qureshi), and $\eta = 3$ or 5 (Higgins). Even if one employs asymptotic tails, substantially larger values of η are required. Our use of real-valued perturbations means, not only in the present application but in general, a gain by a factor of two in the order of the linear-stability system to be solved over the order of the linear system for the real and imaginary parts of complex-valued perturbations used in the traditional approach.

A second advantage of the present analysis over the traditional one is specific to the application at hand. If one uses the buoyancy-force function $B(T)$ defined in (1.3), eliminates p from (1.1) by taking the curl of (1.1b, c), and then linearizes about a base flow, the function $B(T)$ is differentiated twice. But the exponent q in (1.2) lies between 1 and 2. Thus there is a singularity in the coefficients of the linear-stability system obtained at a value of η for which $\Phi(\eta) = R$, and since Φ decreases monotonically from 1 to 0 on $(0, \eta)$ such a value of R exists for every R within (0.0, 0.5), the range of greatest interest. The present approach does not create such a singularity.

In summary, we believe that our approach has advantages that compensate for its disadvantages, both for the present application and potentially in other laminar-fluid-flow problems where multiple steady-state solutions have been found; for example, by Gebhart *et al.* (1983) for a problem involving porous media, by Brady & Acrivos (1981, 1982), Brady (1984), Durofsky & Brady (1984) for flow in an accelerating pipe, and by Gill *et al.* (1985a, b) for surface-tension-driven flow of

η_∞	$\lambda_1(0.151775, 0.050)$	$\lambda_1(0.151788, 0.042)$
40.0	-0.258934×10^{-2}	0.211941×10^{-2}
60.0	-0.261210×10^{-2}	0.208135×10^{-2}
100.0	-0.269591×10^{-2}	0.204128×10^{-2}
150.0	-0.276518×10^{-2}	0.200158×10^{-2}
200.0	-0.281576×10^{-2}	0.196470×10^{-2}

TABLE 3. The dependence of the eigenvalue λ_1, evaluated at $F(\infty) = 0.050$, $R = 0.151775$, upon η_∞ (column 2), and the dependence of the same eigenvalue λ_1, evaluated at $F(\infty) = 0.042$, $R = 0.151788$, upon η_∞ (column 3). All computations done at $\tau = 10.0$.

low-Prandtl-number fluids in various geometries. The method presented here can help to select which of multiple steady states is stable to time-dependent perturbations. The bifurcation diagrams that describe multiple steady-state solutions typically have points of vertical tangency. Usually, where vertical tangencies are found in bifurcation diagrams for time-independent solutions, the real part of one eigenvalue changes sign as one follows the diagram through the point of vertical tangency. Contemporary bifurcation theory is replete with examples: see for example, Iooss & Joseph (1980) or Hassard, Kazarinoff & Wan (1981).

2. Stability analysis and results

We solved the linear system (1.9) together with the suspended trivial equation $\lambda_\eta = 0$ and a sixth boundary condition, specifying either $\tilde{f}(\infty) = 1$ for $R \leqslant 0.15180$ or $\tilde{\phi}(0) = 1$ for $R \geqslant 0.29181$. The eigenvalue problems thus obtained were solved, given $(R, \tilde{f}(\infty))$ or $(R, \tilde{\phi}_\eta(0))$, on a finite interval with boundary conditions at ∞ imposed at $\eta = 200$. We chose $\eta = 200$ since this is the value that is acceptable for the steady-state solutions whose stability is the issue.

The presence of τ in the coefficients of the system (1.9) shows that the formal assumption (1.8) is not mathematically correct. Nevertheless, we have solved the eigenvalue problem (1.9) numerically, for fixed values of τ. We used two totally different computer codes. The first is COLSYS, collocation two-point-boundary-value-problem solver; see Ascher, Christiansen & Russell (1978). The second is BOUNDS, a multiple shooting, two-point-boundary-value-problem solver; see Deuflhard (1980), Deuflhard & Bader (1982), and Bulirsch & Stoer (1966). COLSYS was chosen for its reliability and, in particular, because after solving the steady-state problem for F and Φ using COLSYS, one can store the spline nodes and coefficients, and subsequently evaluate F, Φ and their derivatives in a COLSYS subroutine APPSLN for use in solving (1.9). BOUNDS does not have this ability, since output from BOUNDS consists only of values of solution components at user-specified nodes. Using COLSYS to solve the eigenvalue problem for fixed τ was straightforward. To use BOUNDS we included the subroutine APPSLN from COLSYS in our main driving program to give values of the coefficients in (1.9) at points called by BOUNDS. Both BOUNDS and COLSYS were run in FORTRAN 4.8 on a CYBER 174. The approximate run time per solution was 40 s for each code.

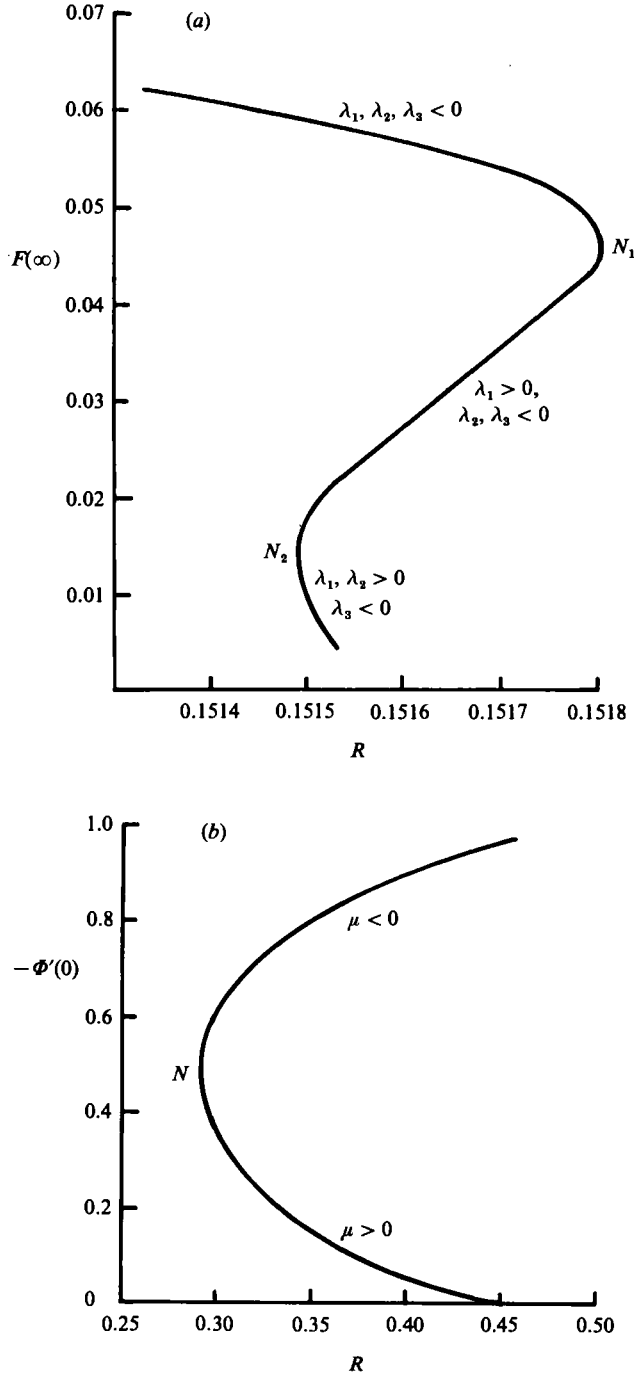

FIGURE 4. Details of the variation of $F(\infty)$ and $-\Phi'(0)$ with R.

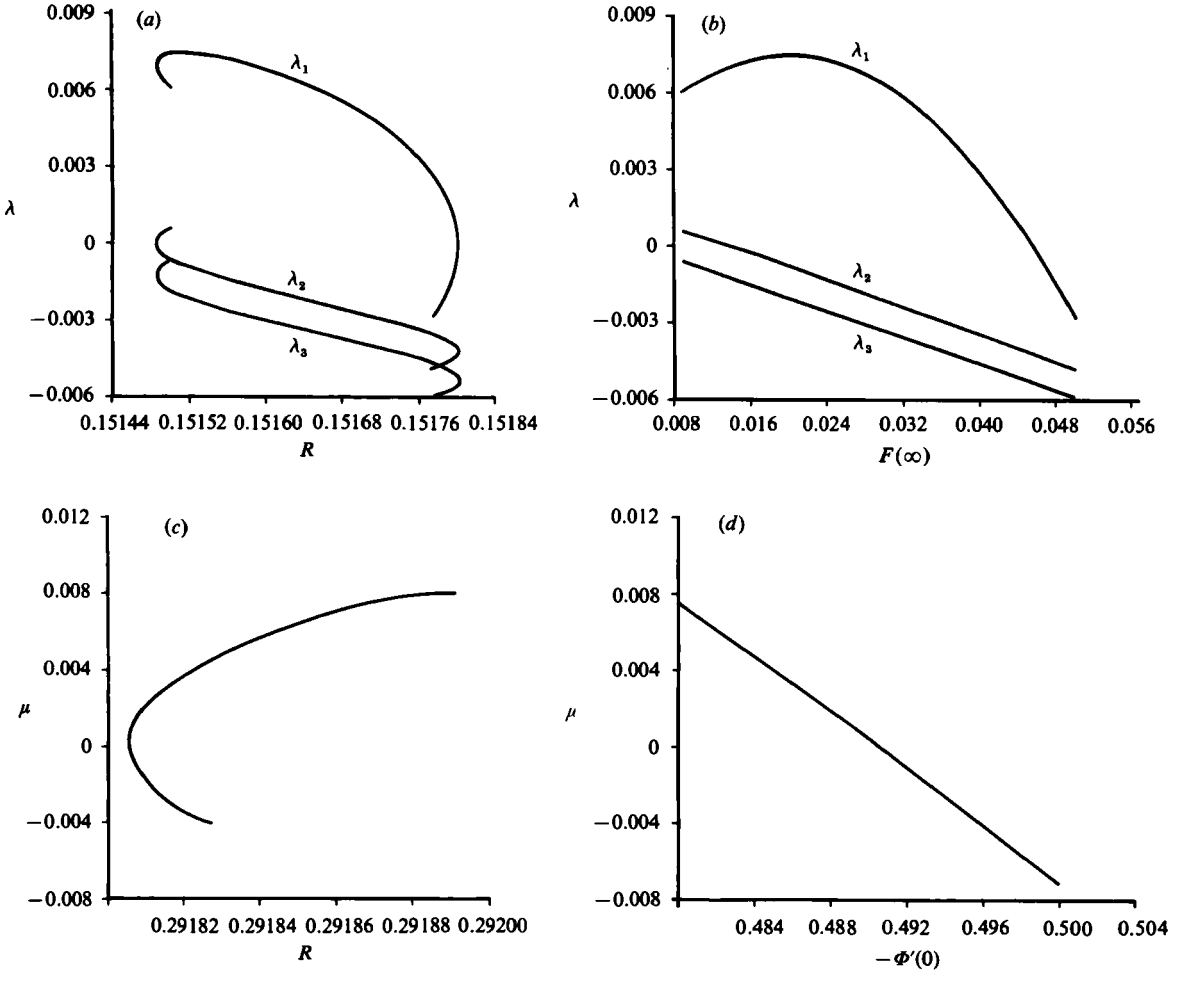

FIGURE 5. (*a*) The variation of $\lambda_i(R, F(\infty))$ $(i = 1, 2, 3)$ with R in the region of largely upflow. (*b*) The variation of $\lambda_i(R, F(\infty))$ $(i = 1, 2, 3)$ with $F(\infty)$ in the region of largely upflow. (*c*) Details of the variation of the eigenvalue $\mu(R, -\Phi'(0))$ with the density-extremum parameter R in the region of largely downflow. (*d*) Variation of the eigenvalue $\mu(R, \Phi'(0))$ with $-\Phi'(0)$ in the region of largely downflow.

3. Bifurcation diagrams and stability

For R in $[0.151486, 0.151801]$ we found and computed three eigenvalues

$$\lambda = \lambda_i(R, F(\infty), \tau) \quad (i = 1, 2, 3)$$

and corresponding eigenvectors

$$(\tilde{f}_i(\eta, \tau), \tilde{\phi}_i(\eta, \tau))^{\mathrm{T}}.$$

Since τ appears explicitly in the coefficients of the linear system (1.9), the eigenvalues and eigenvectors obtained depend parametrically upon τ. However, this dependence is weak; see tables 1 and 2. In fact, the dependence upon τ becomes negligible in the neighbourhood of a 'nose' at which $\lambda = 0$, since τ appears in the governing equations (1.9) only in the combination $\lambda\tau$. This supports the formal assumption (1.8). In

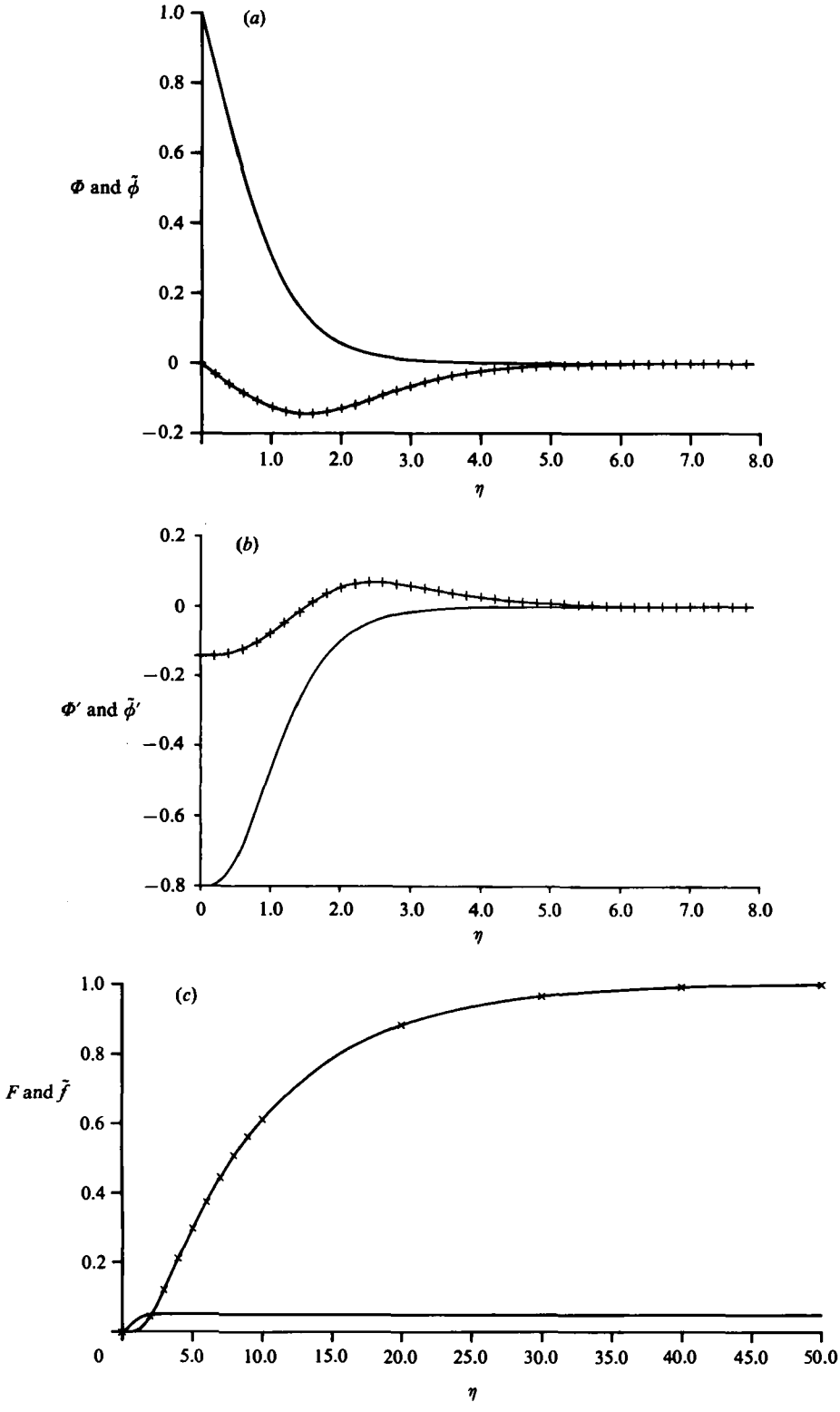

FIGURE 6. For caption see p. 12.

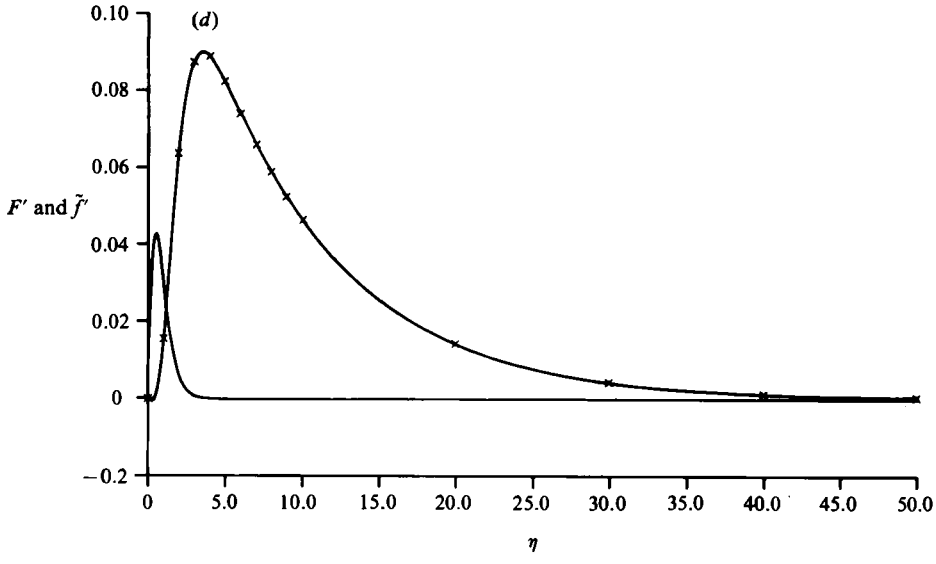

FIGURE 6. Base flows (F, Φ) and corresponding eigenvector components (1st mode; curves marked with crosses) ($\tilde{f}$, $\tilde{\phi}$) at $R = 0.151775$ and $F(\infty) = 0.050$: (*a*) Φ and $\tilde{\phi}$, (*b*) Φ' and $\tilde{\phi}'$, (*c*) F and $\tilde{f}$, (*d*) F'' and $\tilde{f}''$.

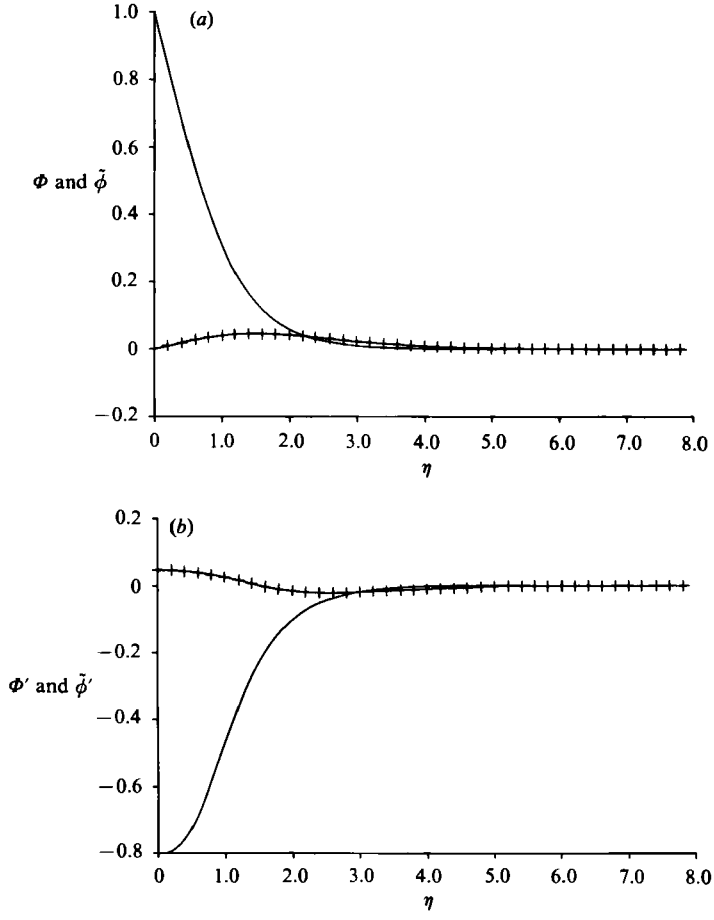

FIGURE 7(*a*) and (*b*). For caption see opposite.

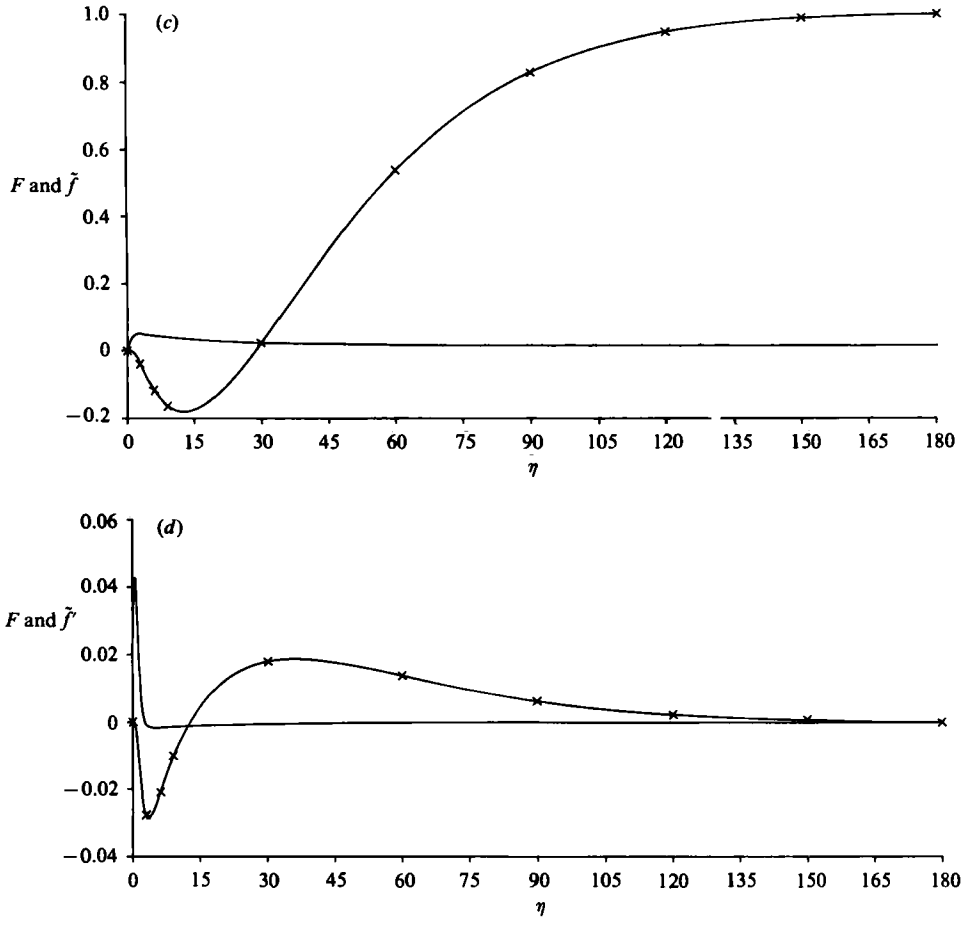

FIGURE 7. Base flows (F, Φ) and corresponding eigenvector components (2nd mode; curves marked with crosses) ($\tilde{f}$, $\tilde{\phi}$) at $R = 0.151486$, $F(\infty) = 0.015$: (*a*) Φ and $\tilde{\phi}$, (*b*) Φ' and $\tilde{\phi}'$, (*c*) F and $\tilde{f}$, (*d*) F' and $\tilde{f}'$.

addition to the dependence upon τ described above, we also tested λ_1 for its response to changes in η_∞ for η_∞ in the interval [40.0, 200.0] (see table 3), for $\tau = 10.0$. We did this for two points $(R, F(\infty))$ close to the nose N_1, namely (0.151775, 0.050) and (0.151788, 0.042). The results show that λ_1 is reasonably insensitive to changes in η_∞. The corresponding eigenvectors change only in the fifth decimal place for these changes in τ and η_∞. For $R > 0.29$, we found and computed just one eigenvalue $\mu(R, -\Phi'(0), \tau)$ for points $(R, -\Phi'(0))$ in the bifurcation diagram 4(*b*). We tested for its sensitivity to τ (see table 2). The dependence on τ is weak, as expected near a 'nose'. We also found μ to be reasonably insensitive to changes in η_∞ (table not shown). In the following computations, the values $\tau = 10.0$ and $\eta = 200.0$ were used. For brevity, we shall not show τ as a parameter in subsequent formulae involving eigenvalues and/or eigenvectors.

The eigenvalues λ_i ($i = 1, 2, 3$) have the following properties. First, $\lambda_1(R, F(\infty)) = 0$ at $(R, F(\infty)) \simeq (0.151801, 0.0455)$, the nose N_1 in the bifurcation diagram figure 3(*a*); $\lambda_1(R, F(\infty)) < 0$ for $F(\infty)$ greater than its value at this nose; and $\lambda_1(R, F(\infty)) > 0$ for $F(\infty)$ less than its value at this nose; see figures 4(*a*), 5(*a*, *b*). Similarly, $\lambda_2(R, F(\infty)) = 0$ at $(R, F(\infty)) \simeq (0.151486, 0.014)$, the nose N_2 in the bifurcation diagram figure 3(*a*); $\lambda_2(R, F(\infty)) < 0$ for $F(\infty)$ greater than its value at N_2; and $\lambda_2(R, F(\infty)) > 0$

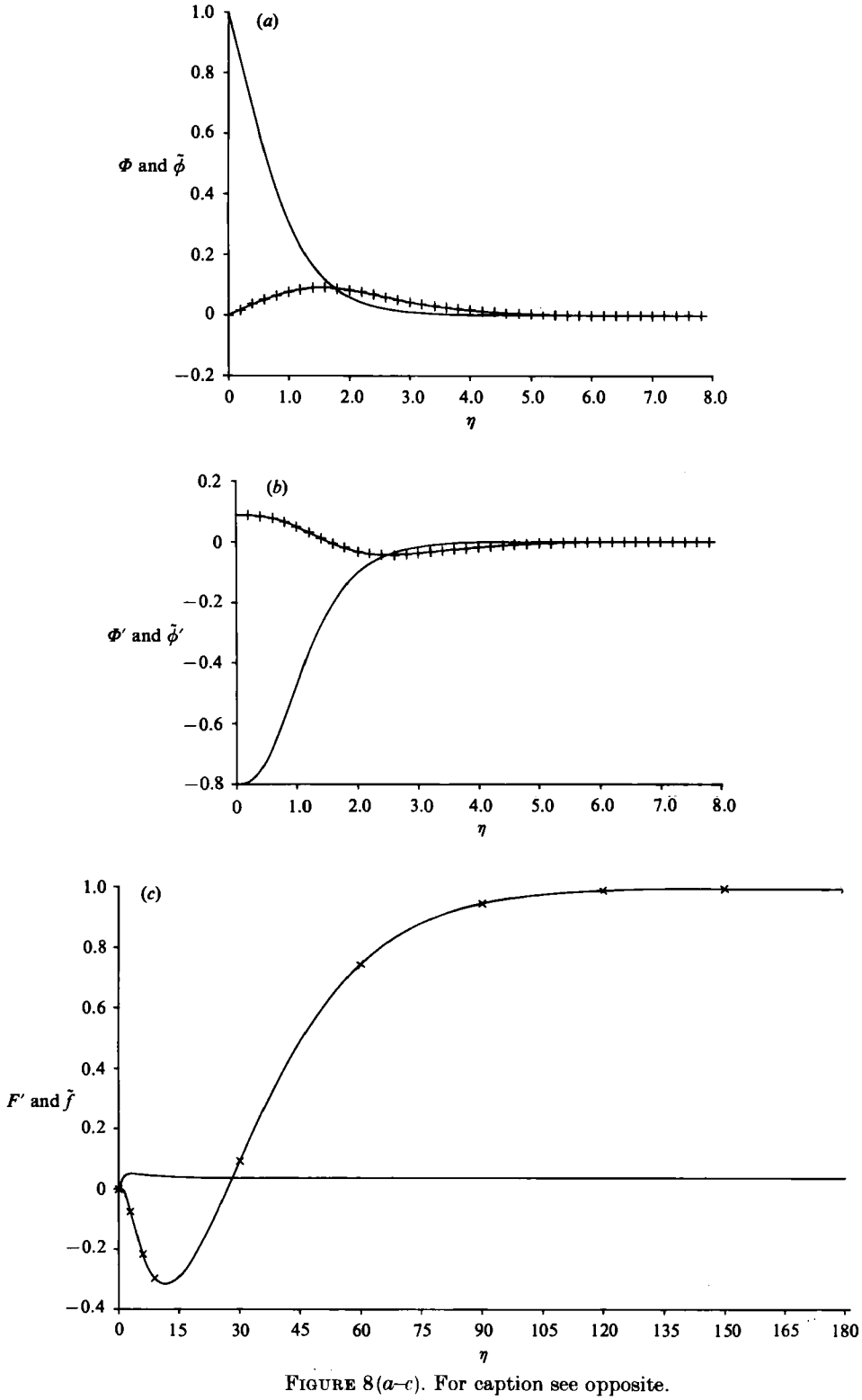

FIGURE 8(*a–c*). For caption see opposite.

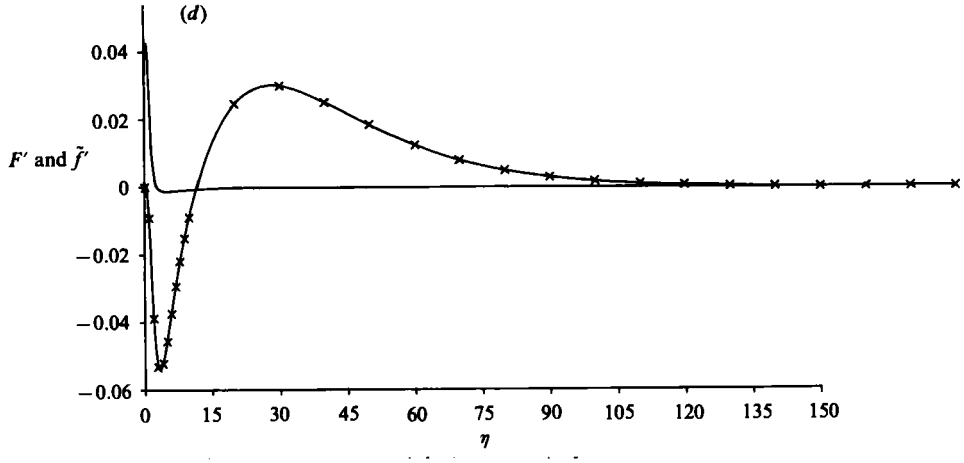

FIGURE 8. Base flows (F, Φ) and corresponding eigenvector components (3rd mode; curves marked with crosses) ($\tilde{f}$, $\tilde{\phi}$) at $R = 0.151735$, $F(\infty) = 0.037$: (*a*) Φ and $\tilde{\phi}$, (*b*) Φ' and $\tilde{\phi}'$, (*c*) F and $\tilde{f}$, (*d*) F', and $\tilde{f}'$.

for $F(\infty)$ less than its value at N_2; see figures 4(*a*), 5(*a*, *b*). The third eigenvalue λ_3 $(R, F(\infty))$ is negative and increasing as $F(\infty)$ decreases from 0.050 to 0.009; see figures 4(*a*), 5(*a*, *b*). We conjecture (based upon figure 5*b*) that there exists a third nose N_3 at a point $(R, F(\infty))$ with $F(\infty) < 0.009$ at which $\lambda_3(R, F(\infty)) = 0$; but we were not able to find such a nose within what we judged to be a reasonable amount of computing effort.

We conjecture that there are infinitely many noses existing for $R < 0.16$ in the complete bifurcation diagram that is partially given in figure 4(*a*) and that corresponding to the ith nose is an eigenvalue $\lambda_i(R, F(\infty))$ that vanishes at the ith nose, is negative for values of $F(\infty)$ greater than its value at this nose, and is positive for all $F(\infty) \geqslant 0$ less than the value of $F(\infty)$ at this nose. We also conjecture that all members of the family of steady-state solutions with $F(\infty)$ greater than its value at the first nose N_1 are stable and all others with values of $F(\infty)$ less than its value at N_1 are unstable. In stating that a steady-state solution is *stable* we mean that small perturbations of the form (1.8) all decay exponentially to 0 as $t \to +\infty$ for each fixed (x, y), and in stating that a steady-state solution is *unstable* we mean that the absolute value of some perturbations of the form (1.8) grows exponentially to $+\infty$ as $t \to +\infty$ for almost all fixed (x, y).

The eigenvalue $\mu(R, -\Phi'(0))$ changes sign at the unique nose N of the bifurcation diagram 4(*b*). The nose lies at approximately (0.291808, 0.493): $\mu < 0$ for $-\Phi'(0)$ greater than its value at this nose, and $\mu > 0$ for $-\Phi'(0)$ less than its value at N; see figures 5(*c*, *d*). For $-\Phi'(0)$ greater than its value at the nose, we believe the steady-state solutions are stable, but lose stability as $-\Phi'(0)$ is decreased beyond 0.493.

To show how the eigenvector components vary with R and how they compare with the corresponding base-flow-solution components, we present figures 6–9. Figures 6–8 cover the situation $R < 0.16$ (largely upflow), while figure 9 is for $R > 0.29$ (largely downflow). Figure 6 shows a solution for $R = 0.15175$, and $F(\infty) = 0.050$, slightly below the first nose seen in figure 3(*a*). The first eigenmode is shown with the base-flow solution because this mode causes the base flow to lose stability as $F(\infty)$ decreases from above to below the first nose. The corresponding plots (not shown) for $R = 0.15175$, but $F(\infty) = 0.048$, slightly below the nose, are virtually identical.

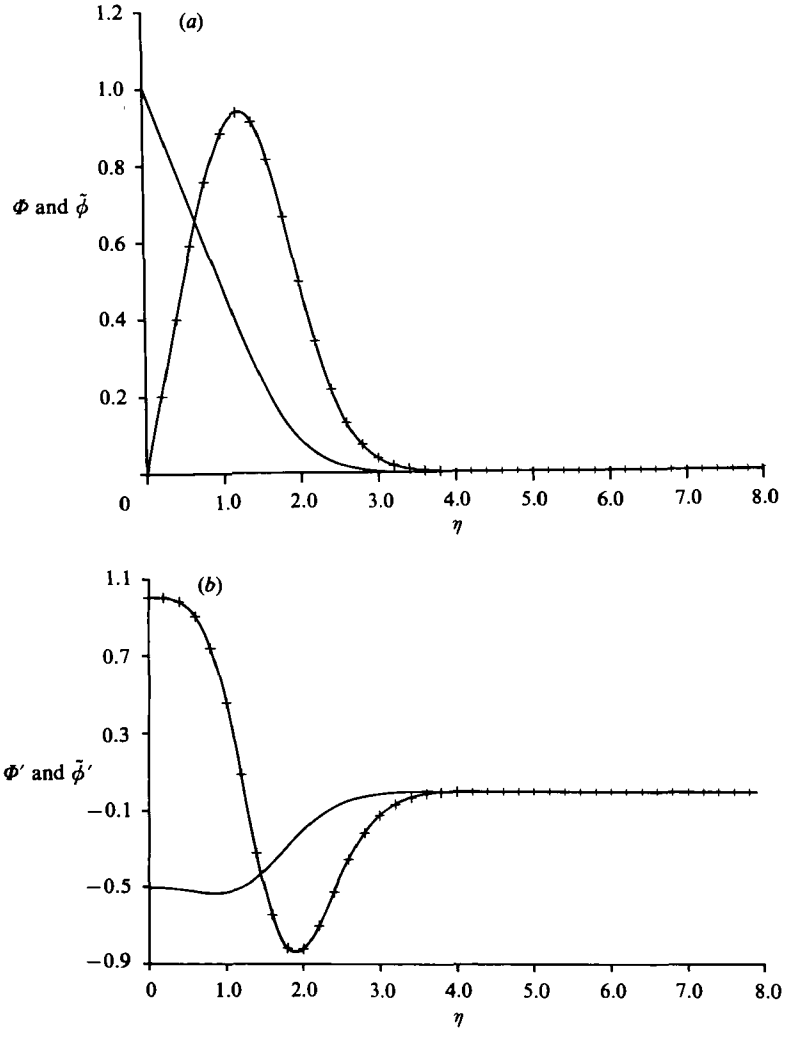

FIGURE 9 (*a*) and (*b*). For caption see opposite.

Analogous statements hold at the other noses. Figure 7 represents a solution for $R = 0.1511486$ and $F(\infty) = 0.015$, slightly above the second nose seen in figure 3 (*a*). The second eigenmode is shown with the base-flow solution since the eigenvalue λ_2 becomes positive as $F(\infty)$ decreases past the second nose. Figure 8 shows the base solution and the corresponding third eigenmode for a value $F(\infty)$ below the first nose but above the second nose. At this value of $F(\infty)$, $\lambda_1 > 0$, $\lambda_2 < 0$ and $\lambda_3 < 0$. λ_3 remains negative as $F(\infty)$ is decreased past the second nose. We conjecture that λ_3 becomes positive past a conjectured third nose. Figure 9 represents a solution on the upper side of the nose in figure 3 (*b*). The eigenmode shown with the base-flow solutions causes the loss of stability as $-\Phi'(0)$ is decreased from above to below the nose.

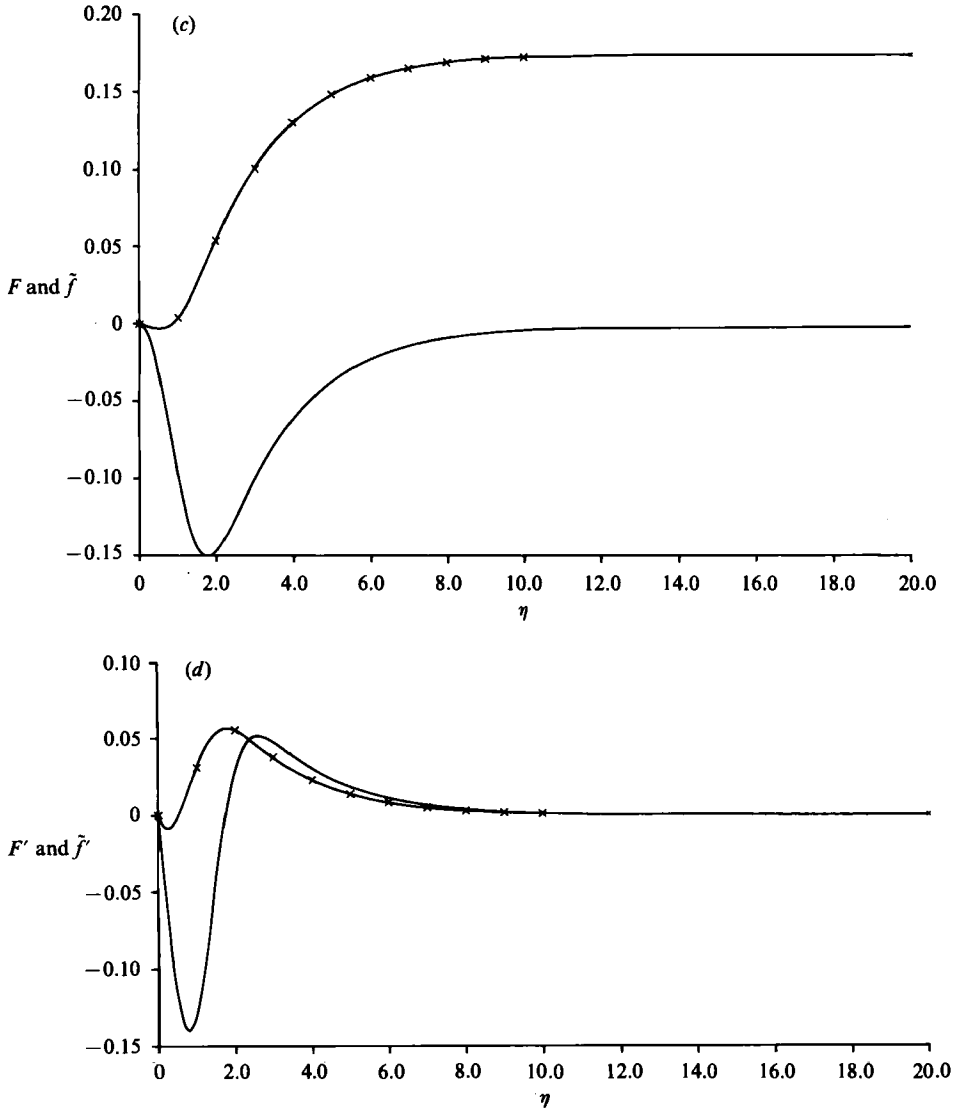

FIGURE 9. Base flows (F, Φ) and corresponding eigenvector components (unique mode found; curves marked with crosses) ($\tilde{f}$, $\tilde{\phi}$) at $R = 0.291878$, $-\Phi'(0) = 0.505$: (*a*) Φ and $\tilde{\phi}$, (*b*) Φ' and $\tilde{\phi}'$, (*c*) F and $\tilde{f}$, (*d*) F' and $\tilde{f}'$.

4. Discussion

We first discuss the behaviour of our perturbations

$$\epsilon\, \mathrm{e}^{\lambda\tau}\begin{pmatrix}\tilde{f}\\ \tilde{\phi}\end{pmatrix}$$

in terms of x, y and t and the vertical and horizontal components of the perturbed velocity $\epsilon\bar{u}(x,y,t)$ and $\epsilon\bar{v}(x,y,t)$ and the perturbed temperature $\epsilon\bar{T}(x,y,t)$. These are

$$\epsilon\begin{pmatrix}\bar{u}(x,y,t)\\ \bar{v}(x,y,t)\end{pmatrix} = \epsilon\, \mathrm{e}^{\lambda\tau(x,t)}\begin{pmatrix}\tilde{u}(x,y)\\ \tilde{v}(x,y)\end{pmatrix} = \epsilon\frac{\nu G}{4x}\mathrm{e}^{\lambda\tau(x,t)}\begin{pmatrix}G\tilde{f}_\eta(\eta)\\ h\tilde{f}_\eta(\eta) - 3\tilde{f}(\eta) + 2\tau\tilde{f}_\eta(\eta)\end{pmatrix}$$

and $$\epsilon\tilde{T}(x,y,t) = \epsilon[(T_0 - T_\infty)\tilde{\phi} + T_\infty].$$

Since $G = \text{const.} \times x^{\frac{3}{4}}$, for fixed t, $\tilde{u}$ grows downstream as $x^{\frac{1}{2}}$ along streamlines $\eta = \text{const.}$, and $\tilde{v}$ decays like $x^{-\frac{1}{4}}$. Our allowed perturbations are not time-periodic, and the observed limiting behaviour of the conventionally studied 'time-periodic' disturbances

$$\epsilon\frac{\nu G}{4\xi}\exp\left[\mathrm{i}(\alpha K_1 x^{\frac{3}{4}} + \beta K_2 x^{\frac{1}{2}}t)\right]\begin{pmatrix} G\tilde{f}_\eta \\ \eta\tilde{f}_\eta - 3\tilde{f} \\ \frac{4x}{G}[(T_0 - T_\infty)\tilde{\phi} + T_\infty] \end{pmatrix}$$

as the frequency β decreases to 0 is that $|\mathrm{Im}\,\alpha|$ becomes very small or zero; see Dring & Gebhart (1969), Hieber & Gebhart (1971), Qureshi (1980) and Higgins (1981), for example. (We write time-periodic in quotation marks because, although β is real, the factor $x^{\frac{1}{4}}$ multiplies t in the exponent above.) Thus, the non-exponential growth downstream of the disturbances that we have derived could be expected and is consistent with the results of others. On the other hand, for fixed (x, y) our real-valued perturbations either grow exponentially with time or decay exponentially with time.

Since reversals occur in the u-component of velocity of some steady-state solutions whose values of $F(\infty)$ are greater than $F(\infty)$ is at N in figure 1 (a) (upflow) as well as in the u-component of velocity of some whose values of $-\Phi'(0)$ are greater than is the value of $-\phi'(0)$ at N in figure 1 (b) (downflow) and since our results indicate that these steady-state solutions may be stable, it is not necessarily true that a steady-state solution which has either an inside or outside reversal in its u-component of velocity (as one looks across the boundary layer) is unstable. Furthermore, such solutions have two points of inflexion in their u-velocity profiles. Thus the 'rule' that more than one point of inflexion in a u-velocity profile implies instability, may be incorrect in the present Problem S.

In summary, the results discussed above lead to the following conclusions: the additional steady-state solutions recently found by El-Henawy *et al.* (1982) are unstable and are unlikely to correspond to physically observable flows. The previously known solutions for $R < 0.152$ and for $R > 0.29$ are likely to be stable; indeed, many of them have been observed (Carey & Gebhart 1981); and we have found no eigenvalues that indicate that they are unstable. These results are important in view of experimental evidence suggesting that there might be physical perturbations of the corresponding flows that make them wander around the steady states; Wilson & Vyas (1979), Carey & Gebhart (1981), Sammakia (1981). Our instability results do not rule out such behaviour.

The authors acknowledge support from the following grants: NSF-MCS8106657 (I.E., B.H. and N.K.) and SUNY RES. FDN.-150-7548-A (I.E.).

REFERENCES

Ascher, U., Christiansen, J. & Russell, R. D. 1978 COLSYS – A collocation code for boundary-value problems. *Codes for Boundary-Value Problems in Ordinary Differential Equations* (ed. G. Goos & J. Hartmanis). Lecture Notes in Computer Science, vol. 76, pp. 164–185. Springer.

Brady, J. F. 1984 Flow development in a porous channel and tube. *Phys. Fluids* **27**, 1061–1067.

BRADY, J. F. & ACRIVOS, A. 1981 Steady flow in a channel or tube with an accelerating surface velocity. An exact solution for the Navier–Stokes equations with reverse flow. *J. Fluid Mech.* **112**, 127–150.

BRADY, J. F. & ACRIVOS, A. 1982 Closed-cavity laminar flows at moderate Reynolds numbers. *J. Fluid Mech.* **115**, 427–442.

BULIRSCH, R. & STOER, J. 1966 Numerical treatment of ordinary differential equations by extrapolation methods. *Numerische Mathematik* **8**, 1–13.

CAREY, V. P. & GEBHART, B. 1981 Visualization of the flow adjacent to vertical ice surface melting in cold pure water. *J. Fluid Mech.* **107**, 37–55.

CAREY, V. P., GEBHART, B. & MOLLENDORF, J. C. 1980 Buoyancy force reversals in vertical natural convection flows in water. *J. Fluid Mech.* **97**, 279–297.

DEUFLHARD, P. 1980 Recent advances in multiple shooting techniques. In *Computational Techniques for O.D.E.* (ed. Caldwell/Sayer), pp. 217–272. Academic.

DEUFLHARD, P. & BADER, G. 1982 Multiple shooting techniques revisited. *Preprint no.* 163. Inst. für Angewandte Math., University of Heidelberg.

DRAZIN, P. G. & REID, W. H. 1981 *Hydrodynamic Stability.* Cambridge University Press.

DRING, R. P. & GEBHART, B. 1968 A theoretical investigation of disturbance amplification in external laminar natural convection. *J. Fluid Mech.* **34**, 551–564.

DRING, R. P. & GEBHART, B. 1969 An experimental investigation of disturbance amplification in external laminar natural convection flow. *J. Fluid Mech.* **36**, 447–464.

DUROFSKY, L. & BRADY, J. F. 1984 The spatial stability of a class of similarity solutions. *Phys. Fluids* **27**, 1068–1076.

EL-HENAWY, I., GEBHART, B., HASSARD, B., KAZARINOFF, N. & MOLLENDORF, J. 1982 Numerically computed multiple steady states of vertical buoyancy-induced flows in cold pure water. *J. Fluid Mech.* **122**, 235–250.

GEBHART, B. 1969 Natural convection flow, instability, and transition. *Trans. ASME* C: *J. Heat Transfer* **91**, 293–309.

GEBHART, B. 1979 Buoyancy-induced fluid motions characteristic of applications in technology. *Trans ASME* I: *J. Fluid Engng* **101**, 5–28.

GEBHART, B., HASSARD, B., HASTINGS, S. P. & KAZARINOFF, N. 1983 Multiple steady-state solutions for buoyancy-induced transport in porous media saturated with cold pure or saline water. *Numer. Heat Transfer* **6**, 337–352.

GEBHART, B. & MOLLENDORF, J. C. 1977 A new density relation for pure and saline water. *Deep-Sea Res.* **24**, 831–848.

GILL, A. E. & DAVEY, A. 1969 Instabilities of a buoyancy driven system. *J. Fluid Mech.* **35**, 775–798.

GILL, W. N., KAZARINOFF, N. D. & VERHOEVEN, J. D. 1985*a* Surface-tension driven flow in low Prandtl number fluids in nearly rectangular and nearly cylindrical floating zones. *Preprint.*

GILL, W. N., KAZARINOFF, N. D. & VERHOEVEN, J. D. 1985*b* Convective diffusion in zone refining of low Prandtl number liquid metals and semiconductors. *Advances in Space Science, Materials Processing of Integrated Circuits, U.C. Davis Meeting, March, 1984* (ed. P. Stroeve). Amer. Chem. Soc. Symposium Series, no. 290, pp. 47–69.

HAALAND, S. E. & SPARROW, E. M. 1973 Stability of buoyant boundary layers and plumes, taking account of non-parallelism of the basic flows. *Trans. ASME* C: *J. Heat Transfer* **95**, 295–301.

HASSARD, B. D., KAZARINOFF, N. D. & WAN, Y.-H. 1981 *Theory and Applications of Hopf Bifurcation* (ed. I. M. James), London Math. Soc. Lecture Notes, vol. 41. Cambridge University Press.

HIEBER, C. A. & GEBHART, B. 1971 Stability of vertical natural convection boundary layers: some numerical solutions. *J. Fluid Mech.* **48**, 625–646.

HIGGINS, J. 1981 Stability of buoyancy induced flow of water near the density extremum, adjacent to a vertical, isothermal surface. Doctoral dissertation, SUNYAB, Buffalo, N.Y.

HWANG, Y. K., KAZARINOFF, N. D. & MOLLENDORF, J. C. 1984 Hydrodynamic stability of multiple steady-states of laminar buoyancy-induced flow adjacent to a vertical plane isothermal surface in cold, pure water. *Preprint.*

IOOSS, G. & JOSEPH, D. D. 1981 *Elementary Stability and Bifurcation Theory.* Springer.

JALURIA, Y. & GEBHART, B. 1974 On transition mechanisms in vertical natural convection flow. *J. Fluid Mech.* **66**, 309–337.

KNOWLES, C. P. & GEBHART, B. 1968 The stability of the laminar natural convection boundary layer. *J. Fluid Mech.* **34**, 657–686.

LIN, C. C. 1955 *The Theory of Hydrodynamic Stability*. Cambridge University Press.

NACHTSHEIM, P. R. 1963 Stability of free-convection boundary layer flows. *NASA TN* D-2089.

POLYMEROPOULOS, C. E. & GEBHART, B. 1967 Incipient instability in free convection laminar boundary layers. *J. Fluid Mech.* **30**, 225–239.

QURESHI, Z. H. 1980 Stability and measurements of fluid and thermal transport in vertical buoyancy induced flows in cold water. Doctoral dissertation, SUNYAB, Buffalo, N.Y.

SAMMAKIA, B. 1981 Transient natural and mixed convection flows and transport adjacent to an ice surface melting in saline water. Doctoral dissertation, SUNYAB, Buffalo, N.Y.

VLIET, G. C. & LIU, C. K. 1969 An experimental study of turbulent natural convection in boundary layers. *Trans. ASME* C: *J. Heat Transfer* **91**, 517–531.

WILSON, N. W. & VYAS, B. D. 1979 Velocity profiles near a vertical ice surface melting into fresh water. *Trans. ASME* C: *J. Heat Transfer* **10**, 313–317.